Doubly-Responsive Hyperbranched Polymers and Core-Crosslinked Star Polymers with Tunable Reversibility

Journal:	*Polymer Chemistry*
Manuscript ID	PY-ART-08-2015-001295.R1
Article Type:	Paper
Date Submitted by the Author:	14-Sep-2015
Complete List of Authors:	Pal, Sunirmal; University of Florida, Department of Chemistry Hill, Megan; University of Florida, Chemistry Sumerlin, Brent; University of Florida, Department of Chemistry;

Polymer Chemistry

ARTICLE

Doubly-Responsive Hyperbranched Polymers and Core-Crosslinked Star Polymers with Tunable Reversibility

Received 00th January 20xx,
Accepted 00th January 20xx

DOI: 10.1039/x0xx00000x

www.rsc.org/

Sunirmal Pal, Megan R. Hill, and Brent S. Sumerlin*

Thermo- and redox-responsive hyperbranched copolymers were prepared by statistical copolymerization of *N*-isopropylacrylamide (NIPAM) and *N,N´*-bis(acryloyl)cystamine (BAC) by reversible addition-fragmentation chain transfer (RAFT) polymerization. Kinetic studies revealed that the molecular weight of the resulting poly(NIPAM-*co*-BAC) gradually increased during the polymerization, and control over molecular weight and degree of branching was demonstrated. The hyperbranched copolymers showed thermoresponsive self-assembly, as determined by dynamic light scattering and turbidity measurements. Hyperbranched poly(NIPAM-*co*-BAC) copolymers were further used for the synthesis of star copolymers by chain extension with *N,N*-dimethylacrylamide. The resulting star copolymers with hyperbranched cores and linear arms were readily degraded under reducing conditions due to the divinyl crosslinker containing a redox-sensitive disulfide linkage. Not only did the disulfide bonds result in macromolecules with redox-responsive behavior, but the ability to cleave and characterize the individual branches of the hyperbranch polymer after synthesis allowed us to confirm the controlled nature of RAFT polymerization in the presence of divinyl compounds.

Introduction

Compared to their linear counterparts, branched architectures, such as hyperbranched polymers and dendrimers, have smaller hydrodynamic volumes and lower solution and melt viscosities. They often exhibit enhanced solubility in a wide range of solvents due to reduced chain entanglement and pronounced end group effects. Branched architectures have compact structures and can accommodate a large number of functional groups for further modification.[1-3] Although the structures of hyperbranched polymers are irregular as compared to those of dendrimers, these two classes of macromolecules share many similar characteristics, and the former can be considered as an alternative to dendrimers in applications such as chemical separation,[4] biosensing,[5] drug delivery,[6, 7] and bioimaging platforms.[8, 9]

Hyperbranched polymers are generally prepared by ring-opening polymerization,[10, 11] step-growth polymerization of AB_x-type monomers,[12] copolymerization of vinyl monomers with divinyl crosslinkers,[13] or copolymerization of vinyl monomers with inimers.[14] Depending on the reaction conditions (*e.g.,* monomer and crosslinker concentration, temperature, stoichiometry), crosslinked gels,[15] microgels,[16] or highly branched (co)polymers[17] can be obtained. Hyperbranched polymers are commonly synthesized using a functional vinyl monomer that can also act as an initiator (*i.e.,* an "inimer"). Polymerization with inimers is often referred to as self-condensing vinyl polymerization (SCVP) and remains one of the most straightforward routes to preparing hyperbranched polymers.[18] Although there have been several reports of SCVP used in combination with controlled/living polymerization, such as reversible addition-fragmentation chain transfer (RAFT),[14, 19, 20] atom transfer radical polymerization (ATRP),[21-23] and nitroxide-mediated radical polymerization[24, 25] to prepare hyperbranched polymers with controlled branched length, many methods involving SCVP may not be readily scalable, due to the complicated and often expensive syntheses of vinyl monomers with specific functional groups capable of initiation.

Another route to hyperbranched polymers makes use of vinyl groups on a divinyl crosslinker, which serves as a branching point during copolymerization with another monomer.[26] Sherrington and co-workers developed versatile and cost-effective routes to the synthesis of hyperbranched or branched polymers using radical polymerization of a vinyl monomer with a divinyl comonomer.[27-30] The same group used dodecanethiol (DDT) as a chain-transfer agent (CTA) to

George & Josephine Butler Polymer Research Laboratory, Center for Macromolecular Science & Engineering, Department of Chemistry, University of Florida, PO Box 117200, Gainesville, FL 32611-7200, USA. E-mail: sumerlin@chem.ufl.edu; Fax: +1 352 392 9741

Electronic Supplementary Information (ESI) available: Experimental details, ^{1}H NMR spectra of *N,N´*-Bis(acryloyl)cystamin (BAC), P(NIPAM-*co*-BAC) (**HBP6**) and P(NIPAM-*co*-BAC)-*star*-PDMA (**HBP7-*star*-PDMA**), Transmittance and Z-average size of polymers with temperature, proposed aggregation characteristics of polymers at above the CP, SEC-refractive index of **HBP5** and **HBP7-*star*-PDMA** after exposure to Bu_3P, SEC-refractive index of P(NIPAM-*co*-MEA) after oxidation, DLS of **HBP10** after degradation by DTT in water at 25 °C and 45 °C, and size exclusion chromatography. See DOI: 10.1039/x0xx00000x

synthesize poly(methyl methacrylate)-branched copolymers by the copolymerization of methyl methacrylate with ethylene glycol dimethacrylate.[31] In many respects, RAFT-mediated copolymerization of a vinyl monomer with a divinyl comonomer is simpler than the combination of SCVP with RAFT, because a diverse set of divinyl monomers is readily available and there is no need to synthesize a new CTA functionalized vinyl monomer. Synthesis of hyperbranched polymers using this method has been reported by Rimmer *et al.*[32] and Perrier and *et al.*[13]

Of particular relevance to the work described in this article, a variety of thermoresponsive hyperbranched (co)polymers, have been prepared by this approach. Among them, poly(*N*-isopropylacrylamide) (PNIPAM) has been extensively investigated for *in vitro* and *in vivo* drug delivery applications.[33, 34] Davis and coworkers synthesized a series of hyperbranched polymers of methacrylated poly(ethylene glycol)s, in which the cloud point (CP) was greatly influenced by the degree of branching.[35] We have reported PNIPAM-based thermoresponsive hyperbranched polymers with tunable solution properties depending on the degree of branching and end group functionality.[14] The goal of this current work is to combine thermoresponsive behavior with reversible-covalent interactions to obtain hyperbranched polymers capable of responding to both temperature and an additional stimulus that can induce degradation.

Reversible-covalent chemistry[36, 37] has often been used as an alternative to supramolecular interactions[38] for self-repairing polymers, and in the synthesis of many macromolecular architectures, including cyclic,[39] star,[40] and hyperbranched polymers,[41] and dendrimers.[42] Among these architectures, reversible-covalent hyperbranched polymers have been prepared utilizing both dynamic disulfide bonds[43] and Diels–Alder[23] linkages, with reversibility of the covalent bonds being induced by a redox and temperature stimulus, respectively. Reversible bonds in hyperbranched polymers show significant potential for stimulus response in many applications and have also been used to confirm the mechanism of SCVP.[23]

The reversible nature of disulfide linkages has been explored in various areas, such as gene transfection,[44] coatings, drug delivery[45, 46] and degradable and self-healing polymers.[47] Disulfide bonds can be reduced to thiols in the presence of a reducing agent (*e.g.,* dithiothreitol (DTT),[48] glutathione (GSH),[43] tris(2-carboxyethyl)phosphine hydrochloride (TCEP),[43] tributylphosphine,[49] and zinc dust[50]) and subsequently may reform disulfide bonds in the presence of an oxidizing agent (*e.g.,* oxygen,[49] hydrogen peroxide,[51] or potassium hexacyanoferrate(III)).[52] Several macromolecular architectures containing reversible disulfide linkages have been prepared, including diblock or multiblock linear polymers,[53] cyclic polymers,[39] self-healing networks,[54] hydrogels,[52] and core/shell hyperbranched polymers.[55] Akiyoshi and coworkers synthesized polysaccharides grafted with short PNIPAM chains to make nanogels through the coupling reactions of thiols by either oxidation or thermal association.[56] Considering previous reports of nanogels being suggested as drug-delivery systems,[57, 58] hyperbranched copolymers containing thiol groups that give rise to thermo- and redox-responsive branched polymers may also be interesting materials for similar applications.[59]

Herein, we report the RAFT synthesis of a series of redox- and thermoresponsive water-soluble hyperbranched copolymers of *N*-isopropylacrylamide (NIPAM) by copolymerization with the disulfide-containing divinyl crosslinker *N,N′*-bis(acryloyl)cystamine (BAC). Hyperbranched copolymers were obtained by RAFT using various comonomer feed ratios to obtain different degrees of branching (DB). The resulting hyperbranched copolymers were used as macro-CTAs for the synthesis of star polymers with redox-responsive hyperbranched cores *via* successive chain extension by RAFT polymerization. The reductive cleavage of branching units with disulfide linkages in the branched polymer led to linear chains with pendant thiol groups. We investigated the effect of temperature on the redox-responsive behavior of disulfide linkages, as well as the reversible degradation and reformation of disulfide bonds in the presence of various reducing and oxidizing reagents. These observations have also been extended to study star polymers with hyperbranched cores.

Results and discussion

Our aim was to synthesize hyperbranched polymers that could respond to two orthogonal stimuli by either supramolecular aggregation or reversible cleavage of covalent bonds. The hyperbranched polymers were dissociated into linear polymer chains and then reconstructed, resulting in either similar or new morphologies, depending on the specific reaction conditions employed. The reversible hyperbranched polymers were synthesized using NIPAM and a disulfide-containing redox-responsive crosslinker, which served as a branching agent. We investigated the effect of temperature on the dissociation and reformation of hyperbranched polymers through the redox cycle.

Hyperbranched Polymer Synthesis and Characterization

The copolymerization of a vinyl monomer with a divinyl comonomer *via* RAFT sometimes leads to insoluble gels, depending on the CTA and crosslinker ratio. Liu *et al.* observed that the copolymerization of 2-(2-methoxyethoxy)ethyl methacrylate with di(ethylene glycol)dimethacrylate (DEGDMA) formed a gel when the feed ratio was [CTA]/[DEGDMA] < 0.5.[13] In this work, gelation of the copolymerization reaction was observed visually when RAFT polymerization was carried out with NIPAM and the disulfide containing degradable crosslinker BAC in the presence of 4-cyano-4-(dodecylsulfanylthiocarbonyl)-sulfanyl pentanoic acid (CDP) as CTA and 2,2′-azobisisobutyronitrile (AIBN) as initiator at a feed ratio of [NIPAM]:[BAC]:[CDP]:[AIBN] = 100:6:1:0.2. Therefore, further studies required that the feed ratio of [CDP]:[BAC] be kept below 1:6 to avoid gelation during polymerization.

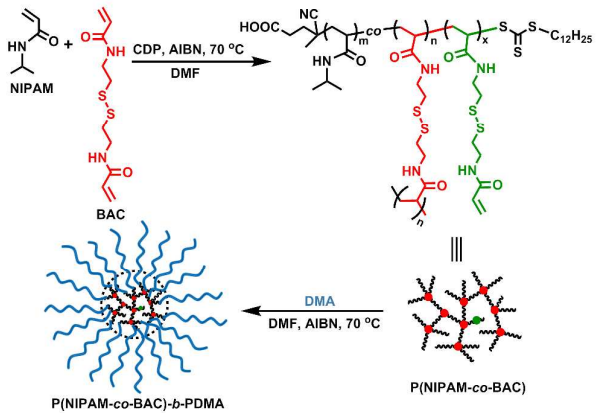

Scheme 1 Synthesis of hyperbranched copolymer P(NIPAM-*co*-BAC) and corresponding star polymer with *N,N*-dimethylacrylamide (DMA) by RAFT.

Successful synthesis of hyperbranched [poly(*N*-isopropylacrylamide-*co*-*N,N´*-bis(acryloyl)cystamine) [P(NIPAM-*co*-BAC) copolymers was accomplished by the RAFT copolymerization of NIPAM with BAC in the presence of CDP as the CTA (Scheme 1). The copolymerization reaction was conducted with nine different molar feed ratios of [NIPAM]:[BAC]:[CDP]:[AIBN]. The details of the copolymerizations are summarized in Table 1.

The structure of P(NIPAM-*co*-BAC) was confirmed by ^{1}H NMR spectroscopy (Supporting Information, Fig. S2), and the molecular weight (M_n) and molecular weight distributions ($Đ$) were determined by SEC (Fig. 1). The $M_{n,SEC}$ of the hyperbranched polymers with feed compositions [NIPAM]:[BAC]:[CDP] = 10:1:1 (**HBP1**) and 100:5:1 (**HBP10**) varied from 8,400 to 1,372,000 g/mol with corresponding $Đ$ of 2.10 and 7.53, respectively (Table 1).

RAFT Polymerization Kinetics

The polymerization of NIPAM and BAC showed pseudo-first-order kinetics (Fig. 2A), indicating a constant concentration of propagating radicals as expected for RAFT polymerizations. An induction period of 20-25 min was observed, which could be a result of the presence of trace amounts of impurities or slow initialization.[60] Fig. 2B shows the relationship between $M_{n,SEC}$ and the monomer conversion for the synthesis of **HBP3**, **HBP4**, **HBP5**, and **HBP6** at similar levels of monomer conversion. Most notably, the evolution of molecular weight with converstion of **HBP8** shows a dramatic increase in molecular weight above 80% conversion. It is expected that RAFT polymerization of divinyl monomers to form hyperbranched polymers will result in higher $M_{n,SEC}$ than conventional RAFT, as the incorporation of the divinyl monomer generates branching points. As a result, the polymerization first forms linear polymers early in the copolymerization before leading to significant branching as the residual side-chain vinyl units of begin undergoing attack by the propagating radical chain ends.[26] The increased occurrence of polymer-polymer addition reactions late in the polymerization results in rapid increases in molecular weight, as exemplified by **HBP8**. As expected, the M_n increases with increasing [BAC]:[CDP] ratio as the density of branching points increases (Table 1).

Table 1 Results of the synthesis of P(NIPAM-*co*-BAC) hyperbranched copolymer by RAFT polymerization of NIPAM and BAC at 70 °C in DMF under various reaction conditions

Sample Name	[NIPAM]:[BAC]:[CDP]:[AIBN]	Time (min)	Conversion (%)[a]	$M_{n,Theo}$ (g/mol)	$M_{n,SEC}$[b] (g/mol)	$Đ$[b]	DB[c]	RB[d]
PNIPAM	100:0:1:0.2	110	87	10,300	12,700	1.12	-	-
HBP1	10:1:1:0.2	300	99	1,800	8,400	2.10	0.253	3.950
HBP2	25:1:1:0.2	300	99	3,500	17,400	1.61	0.128	7.810
HBP3	100:1:1:0.2	100	84	10,100	17,700	1.21	0.031	32.25
HBP4	100:2:1:0.2	100	83	10,200	20,800	1.47	0.034	29.41
HBP5	100:3:1:0.2	100	82	10,150	24,200	1.70	0.049	20.40
HBP6	100:4:1:0.2	100	85	10,950	32,200	2.33	0.060	16.66
HBP7	100:4:1:0.2	360	97	12,400	45,200	4.29	-	-
HBP8	100:5:1:0.2	360	97	12,650	160,000	5.27	-	-
HBP9	100:5:1:0.2	420	96	12,200	334,400	5.71	-	-
HBP10	100:5:1:0.2	390	98	12,350	1,372,000	7.53	-	-
HBP11	100:6:1:0.2	180	Gel	-	-	-	-	-

[a]Calculated by ^{1}H NMR spectroscopy. [b]Number-average molecular weight ($M_{n,SEC}$) and molecular weight distribution ($Đ$) obtained by size-exclusion chromatography (SEC). [c]Degree of branching (DB) calculated from ^{1}H NMR spectroscopy. [d]Average repeat units per branch (RB) = 1/Degree of branching.

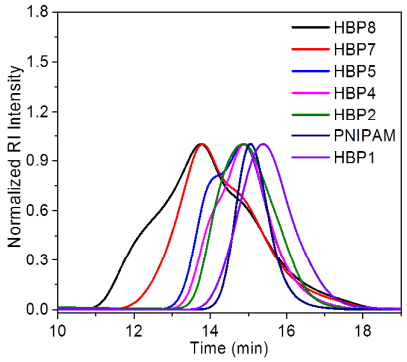

Fig. 1 SEC-refractive index traces of P(NIPAM-*co*-BAC) hyperbranched copolymers obtained by RAFT copolymerization of NIPAM and BAC at different feed ratios.

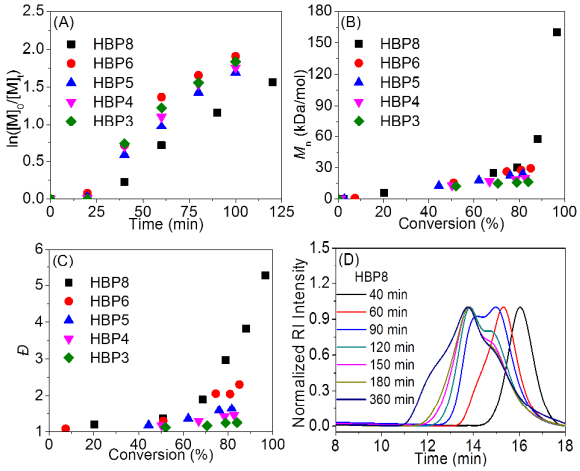

Fig. 2 (A) Pseudo-first-order kinetics plots for the RAFT polymerization of NIPAM and BAC at different feed ratios of [NIPAM]:[BAC]:[CDP] in DMF at 70 °C; (B) corresponding M_n vs. monomer conversion; (C) $Đ$ as a function of monomer conversion; (D) SEC-refractive index traces as a function of time for the synthesis of **HBP8**.

The evolution of molecular weight dispersity during the hyperbranch polymerizations is shown in Fig. 2C, where the values are observed to increase with increasing monomer conversion. Fig. 2D displays the molecular weight distributions of **HBP8** as a function of time. The SEC refractive index trace moves to lower elution time and broadens as branching occurs during polymerization. The molecular weight distribution of **HBP8** in Fig. 1 shows that, with increasing [BAC]:[NIPAM] ratio, the molecular weight distribution of the hyperbranched polymer becomes wider, consistent with the formation of branched polymers.

Branching Unit Calculation for the Hyperbranched Polymer

The degree of branching (DB) is an important parameter to describe the fraction of branching units in macromolecules. DB relationships have been derived for polycondensation,[61, 62] RAFT[63] and SCVP[64] polymerization. In this work, ^{1}H NMR spectroscopy was used to calculate the DB from the number of terminal (*T*), linear (*L*) and branching (*B*) units, according to following equation:[65]

$$DB = \frac{B+T}{B+T+L} \quad (2)$$

where each branching unit generates an extra branch through chain growth with crosslinker. For hyperbranch polymers prepared by RAFT polymerization, this formula can be modified to account for the presence of end groups that originate from the Z- and R-groups of the RAFT agent to give eqn 2.

$$DB = \frac{B + T_R + T_Z}{B + T_R + T_Z + L} \quad (3)$$

where T_R and T_Z signify the number of terminal units in the polymer that originate from the R- and Z-groups in the RAFT agent (Scheme 2). Since the number of R and Z groups should be equal and because the Z-groups are readily visible by ^{1}H NMR spectroscopy, this equation can be further simplified to obtain eqn 3:

$$DB = \frac{B + 2T_Z}{B + 2T_Z + L} \quad (4)$$

Therefore, the degree of branching of P(NIPAM-*co*-BAC) was calculated using the peak area of -C*H*$(CH_3)_2$ in the linear NIPAM units at 3.99 ppm, the S-C*H*$_2$ methylene unit of the dodecyl Z-group at 3.33 ppm, and the methylene proton of the crosslinker (S-S-C*H*$_2$) at 2.91 ppm. The results are shown in Table 1. The highest DB (HBP1) was 0.253 for the feed ratio of [NIPAM]:[BAC] = 10:1 with the average repeat units per branch (RB) = 3.95, whereas the feed ratio of 100:1 led to DB = 0.031 in HBP3 and the corresponding RB = 32.25. These results clearly show that the DB gradually increases with increasing crosslinker concentration in the feed ratio of NIPAM and BAC. According to the definition of DB, high molecular weight linear polymers have a DB that approaches zero, and perfectly branched macromolecules (e.g., dendrimers) have DB = 1.[65] The DB values obtained here indicate branched architecture.

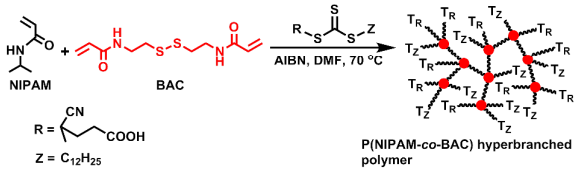

Scheme 2 Generation of two branched units from each divinyl crosslinker for the synthesis of P(NIPAM-*co*-BAC).

Star Polymer Synthesis by Chain Extension Polymerization of P(NIPAM-*co*-BAC) with DMA *via* RAFT

Star polymers are usually synthesised by either core-first[66, 67] or arm-first[40, 41] strategies. In the core-first method, the multifunctional core is usually made by multi-step organic synthesis and subsequently used to form the arms from the core. The disadvantages of this approach are the often numerous steps to synthesize the multifunctional cores and the difficulty in purification, leading to extended synthesis times and potentially lower yields. In the arm-first method, the star is prepared by the reaction of functional linear arms with multifunctional crosslinkers. The disadvantage of this method lies in the uncertainty of the number of arms incorporated and the difficulty in purification of the desired star polymers with the targeted number of arms. Many of these drawbacks can be avoided by the synthesis of star polymers from a chain-end functional hyperbranched core. To obtain hyperbranched star copolymers, P(NIPAM-*co*-BAC) was used as a macro-RAFT agent to synthesize P(NIPAM-*co*-BAC)-*star*-poly(*N,N*-dimethylacrylamide) (P(NIPAM-*co*-BAC)-*star*-PDMA) by subsequent RAFT polymerization of DMA. In this work, five different star copolymers were prepared by RAFT in DMF at 70 °C. The feed ratio of [DMA]:[P(NIPAM-*co*-BAC)-macro-CTA]:[AIBN], the $M_{n,SEC}$ of hyperbranched star copolymers, and the molecular weight dispersity are summarized in Table 2. The SEC-refractive index traces of the resulting star copolymers [P(NIPAM-*co*-BAC)-*star*-DMA] shifted toward lower elution time, as compared to the corresponding hyperbranched polymers (Fig. 3). For example the M_n of **HBP5**, **HBP6**, and **HBP7** (24,200, 32,200 and 45,200 g/mol, respectively) shift to 51,200, 65,600, and 162,300 g/mol, for **HBP5-*star*-PDMA**, **HBP6-*star*-PDMA**, and **HBP7-*star*-PDMA** star polymers, respectively. The typical ^{1}H NMR spectrum (Supporting Information, Fig. S3) of star copolymers shows characteristic resonance signals for NIPAM and DMA units.

The theoretical average number of linear PDMA arms in the P(NIPAM-*co*-BAC)-*star*-PDMA hyperbranched star copolymers can be calculated using the $M_{n,SEC}$ values of the star polymers and the hyperbranched macro-RAFT agent and the conversion of DMA (Equation 1). First, the $M_{n,theo}$ of PDMA was calculated as the theoretical molecular weight at a given conversion expected for an analogous linear homopolymerization of DMA. The number of arms of stars is presented in Table 2.

$$\#\ \mathbf{arms} = \frac{\boldsymbol{M_n}\ \mathbf{of\ HB\ star\ polymer} - \boldsymbol{M_n}\ \mathbf{of\ HB\ macro\ RAFT\ agent}}{\mathbf{Theoretical}\ \boldsymbol{M_n}\ \mathbf{of\ PDMA}} \quad (1)$$

The polymerization kinetics for star polymer synthesis was investigated by analysing the polymerization reaction mixture withdrawn from the reaction vessel at specified times to determine the monomer conversion. Monomer conversions were calculated using ^{1}H NMR analysis, where the intensity of the peak for DMF at 7.98 ppm (internal standard) was compared to the intensities of the vinyl protons of DMA at 6.22 and 5.65 ppm at different time intervals. Pseudo-first-

Table 2 Results of the synthesis of P(NIPAM-*co*-BAC)-*star*-PDMA hyperbranched star copolymers by RAFT polymerization at 70 °C in DMF

Polymer	[DMA]:[Macro-CTA]:[AIBN]	Time (min)	Conversion (%)[a]	$M_{n,\ Theo}$[b] (g/mol)	$M_{n,\ SEC}$[c] (g/mol)	$Đ$[c]	Number of arms
HBP3-*star*-PDMA	100:1:0.2	75	88	8,700	28,100	1.61	1.19
HBP4-*star*-PDMA	100:1:0.2	75	87	8,600	36,600	1.74	1.84
HBP5-*star*-PDMA	100:1:0.2	75	85	8,400	51,200	2.14	3.21
HBP6-*star*-PDMA	100:1:0.2	75	87	8,600	65,600	3.82	3.88
HBP7-*star*-PDMA	200:1:0.2	600	99	19,700	162,300	4.17	5.94

[a]Calculated by ^{1}H NMR spectroscopy. [b]Theoretical molecular weight of PDMA polymer arms: $M_{n,Theo} = \frac{[DMA]}{[\text{Macro RAFT agent}]} \cdot$MW of DMA $\cdot$Monomer Conversion. [c]Obtained by SEC in *N,N*-dimethylacetamide(DMAc).

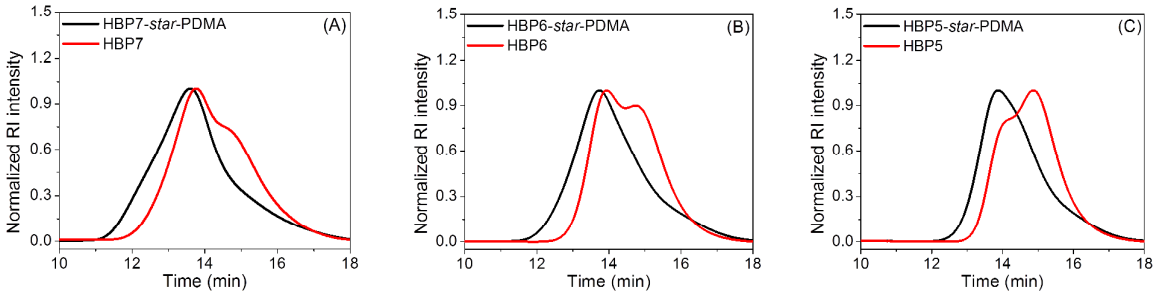

Fig. 3 SEC-refractive index traces of (A) **HBP7** macro-CTA and **HBP7-*star*-PDMA**, (B) **HBP6** macro-CTA and **HBP6-*star*-PDMA**, and (C) **HBP5** macro-CTA and **HBP5-*star*-PDMA**.

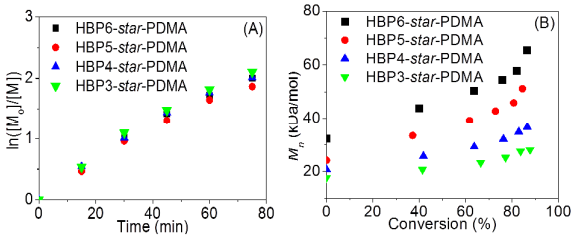

Fig. 4 (A) Pseudo-first-order kinetics plots for RAFT polymerization of P(NIPAM-*co*-BAC)-macro-CTAs with DMA in DMF at 70 °C; (B) corresponding M_n vs. monomer conversion.

order kinetics were observed throughout the polymerization, even at high conversion (Fig. 4A). Figure 4B shows a linear relationship between $M_{n,SEC}$ and monomer conversion for the hyperbranched star polymerization up to 86% conversion. No gelation was observed throughout the polymerization (even close to 100% conversion) during the synthesis of HBP7-*star*-PDMA (Table 2), which is consistent with the successful synthesis of P(NIPAM-*co*-BAC)-*star*-PDMA by the core-first approach and subsequent chain extension of the hyperbranched macro-CTA by RAFT polymerization.

Solution Behavior of Hyperbranched Copolymers

The thermo-responsive behavior of PNIPAM and P(NIPAM-*co*-BAC) was examined in aqueous media as a function of temperature using a UV-Vis spectrophotometer for turbidity measurements at 500 nm. The cloud point (CP) of a polymeric material is defined here as the temperature corresponding to 10% reduction of transmittance, and it depends on the solution concentration, molecular weight of the polymer, and chain end functionality.[14] The CP of PNIPAM was reported previously to be 32 °C.[68] As expected, the CP values decrease (Supporting Information, Fig. S4) with increasing amounts of hydrophobic BAC and CTA-derived dodecyl end groups units in the P(NIPAM-*co*-BAC) copolymer and, hence, with increasing degree of branching as summarized in Table 3. For example, CP of **HBP3** ([NIPAM]:[BAC] = 100:1 feed ratio) was found to be 28.9 °C, whereas CP of **HBP8** ([NIPAM]:[BAC] = 100:5 feed ratio) was obtained at 25.5 °C.

We also investigated the temperature-dependent aqueous solution behavior of the branched P(NIPAM-*co*-BAC) by dynamic light scattering (DLS). Desolvation of the polymers above the CP resulted in the formation of large particles due to intermolecular aggregation. In agreement with the turbidity results, the CPs determined by DLS for the P(NIPAM-*co*-BAC) copolymers are less than that of the linear PNIPAM (Supporting Information, Fig. S5). Significantly, we observed that the aggregation size of the hyperbranched polymers above the CP decreased with increasing DB and decreasing RB (Table 1). The sizes of the aggregated hyperbranched polymers measured at 35 °C are compared in Table 3. On the basis of DLS, the proposed aggregation characteristics of P(NIPAM-*co*-BAC) hyperbranched polymers dictate that their CP decreaeses with increasing branching density (Supporting Information, Fig. S6).

Table 3. Aqueous solution properties of linear PNIPAM and hyperbranched copolymers

Polymer	$CP_{Turbidity}$ (°C)[a]	CP_{DLS} (°C)[b]	D_h (nm) at 35 °C[c]
PNIPAM	30.1	31.0	215
HBP3	28.9	29.9	134
HBP4	28.2	29.3	87
HBP5	26.6	27.5	65
HBP6	26.1	26.8	50
HBP8	25.5	27.0	33

CP measured by [a]turbidity and [b]dynamic light scattering (DLS). [c]Average hydrodynamic diameters of linear and hyperbranched polymers obtained by DLS at 35 °C.

Study of Dynamic Reversible Dissociation and Formation of Hyperbranched Polymers

The degradation of P(NIPAM-*co*-BAC) was investigated by SEC and DLS after exposing the polymers to reducing agents capable of cleaving the disulfide bonds in the BAC units, including, dimethylphenylphosphine (DMPP), tri-*n*-butylphosphine (Bu_3P) and dithiothreitol (DTT). The disulfide linkages were reduced more rapidly to thiol functionalized polymers when DMPP or Bu_3P was used as the reducing agent instead of DTT. Initially, we tested the degradation of **HBP5** in DMAc using Bu_3P as reducing agent ([Bu_3P]/[S-S] = 5 equiv, reaction time = 45 min). SEC traces of **HBP5** after reduction by either Bu_3P or DMPP were shifted to higher retention time (Supporting Information, Fig. S7) as expected. The $M_{n,SEC}$ of the polymer was reduced to 12,850 g/mol from the original 24,200 g/mol before Bu_3P treatment. Interestingly, the $M_{n,SEC}$ value for **HBP5** after degradation was similar to the $M_{n,Theo}$ (10,150 g/mol) calculated from the monomer conversion assuming linear homopolymerization of NIPAM monomer *via* controlled RAFT polymerization (Table 1). Once again, the results indicate that formation of a hyperbranched polymer of NIPAM is controlled by RAFT, as $M_{n,Theo}$ matched with the $M_{n,SEC}$ of the degraded polymer. Therefore, not only did the disulfide bonds result in hyperbranched macromolecules with redox-responsive behavior, but the ability to cleave and characterize the individual branches of the hyperbranch polymer after synthesis allowed us to confirm of the controlled nature of RAFT polymerization in the presence of divinyl compounds. These results compare favorably with our previous investigations into the mechanism of SCVP with reversible-covalent ATRP inimers.[23] A similar result was observed (Supporting Information, Fig. S7) for the degradation of the (S-S) bond in **HBP5** with DMPP as the reducing agent. Hence, Bu_3P and DMPP were demonstrated to be efficient reducing agents for decomposing the disulfide linkages in the hyperbranched polymers to form their respective linear copolymers.

The disulfide bonds in **HBP10** were also cleaved by DTT in *N,N*-dimethylacetamide (DMAc) under N_2 ([DTT]/[S-S] = 12.6 equiv), and the kinetics of the dissociation was studied using DLS and SEC. For the kinetics study, aliquots were withdrawn periodically for DLS and SEC analysis. The size of the polymers progressively decreased from 60 to 8 nm (Fig. 5A) with time, and the SEC curves shifted sequentially to higher retention times (Fig. 5C). The $M_{n,SEC}$ of **HBP10** decreased from 1,372,000 to 34,400 g/mol, as shown in Fig. 5B. Thus, SEC and DLS results clearly show that the (S-S) bonds are degraded successfully by DTT in DMAc.

After the successful degradation study of disulfide functional hyperbranched polymers in an organic solvent, we decided to conduct the same study in aqueous medium under N_2 atmosphere using DTT as the reducing agent. Since P(NIPAM-*co*-BAC) displays thermoresponsive behavior in aqueous solution, we investigated the degradation reaction both above the CP (45 °C) and below the CP (25 °C) of the hyperbranched polymers. The size of the **HBP10** changed from its original 52 nm to 23 nm at 25 °C and 24 nm at 45 °C after 5 h (Supporting Information, Fig. S8). Thus, we have successfully demonstrated the degradation of disulfide bonds in both an organic solvent (using Bu_3P, DMPP and DTT) and in aqueous solution (using DTT).

After confirming successful reductive cleavage of the disulfide-containing hyperbranched polymers, we decided to investigate the re-formation of disulfide bonds from the linear poly(*N*-isopropylacrylamide-*co*-*N*-(2-mercaptoethyl)acrylamide) (P(NIPAM-*co*-MEA) fragments that resulted from degradation. We used excess Bu_3P ([Bu_3P]:[S-S] = 7:1, reaction time = 24 h, under N_2 in THF) to reduce the disulfide bonds of P(NIPAM-*co*-BAC), and the thiol-containing linear P(NIPAM-*co*-MEA) polymers were isolated using dialysis to remove excess Bu_3P. However, it was difficult to isolate completely reduced and dried linear polymer, due to reformation of the disulfide linkages by trace amounts of O_2 in water, even under acidic conditions (pH ≈ 3) and under N_2 atmosphere. As a result, we isolated a mixture of P(NIPAM-*co*-MEA) and P(NIPAM-*co*-BAC) polymers, which had higher molecular weight than expected for linear polymers of P(NIPAM-*co*-MEA). The $M_{n,SEC}$ of the isolated polymers was 34,000 g/mol ($Đ$ = 1.44). Similarly, disulfide bonds in P(NIPAM-*co*-BAC)-*star*-PDMA star polymers were also decomposed by excess Bu_3P in THF and dialysed against acidic water (pH ≈ 3) for two days under N_2 atmosphere. The $M_{n,SEC}$ of the isolated polymers was 49,300 g/mol ($Đ$ = 1.47). The SEC traces was shifted towards higher elution time (Supporting Information, Fig S9) that the linear thiol-containing [P(NIPAM-*co*-MEA)-*b*-PDMA] block copolymer was obtained, which was used for further studies of the re-formation of disulfide bonds.

Reformation of hyperbranched polymers from linear P(NIPAM-*co*-MEA) was carried out by oxidative coupling in the presence of $K_3[Fe(CN)_6]$[52] in water at 25 and 45 °C to obtain disulfide-containing P(NIPAM-*co*-BAC) branched polymers (Scheme 3). Samples were withdrawn at different time intervals for the reaction at 25 °C, and the water was removed by lyophilization before determining the molecular weight by

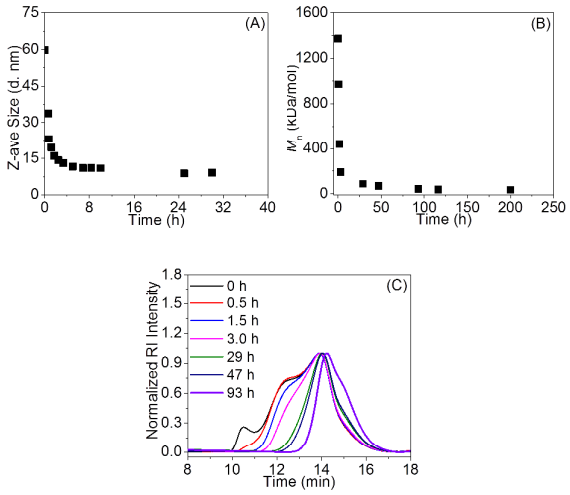

Fig. 5 Reductive cleavage of disulfide bonds in **HBP10** by DTT. (A) Kinetics of degradation in size determined by DLS; (B) Kinetics of degradation in molecular weight determined by SEC; (C) SEC-refractive index traces showing the progress of reaction with time.

SEC. The SEC trace of the polymers shifted towards lower elution time (Supporting Information, Fig. S10) with increasing reaction time, while the $M_{n,SEC}$ shifted from 34,000 to 142,600 g/mol, indicating interpolymer coupling *via* disulfide bond formation. Interestingly, we observed formation of a microgel when the disulfide coupling reaction was carried out at 45 °C, presumably due to the aggregation of a large number of thiol-

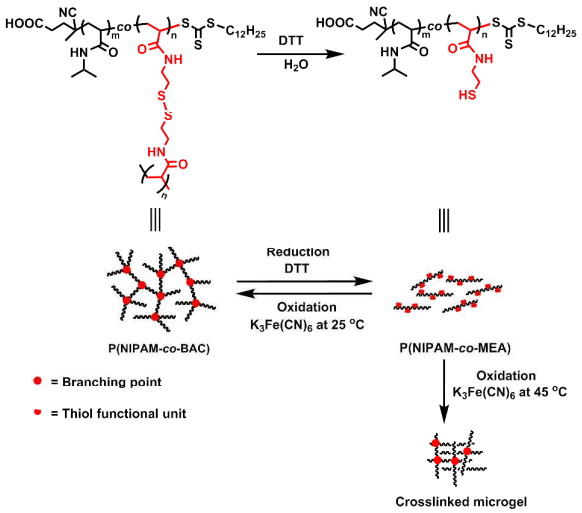

Scheme 3 Redox-responsive reversible disassembly and reassembly of disulfide- containing hyperbranched polymers at 25 °C, and microgel formation at 45 °C by coupling of thiol functional polymers obtained after degradation.

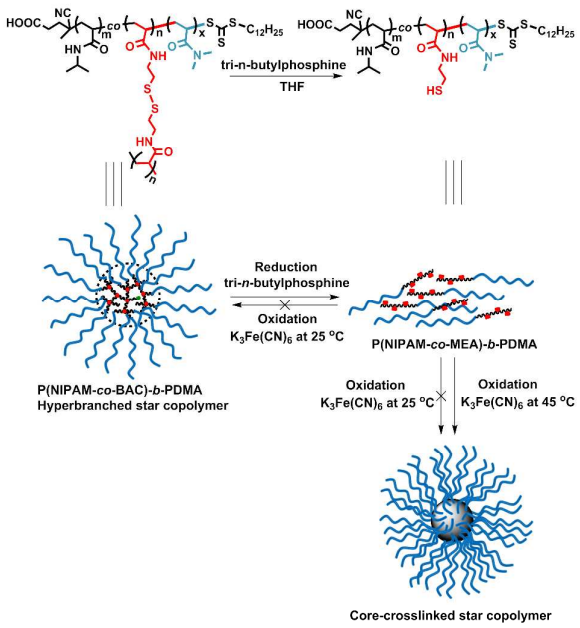

Scheme 4 Degradation of hyperbranched star copolymer and formation of core-crosslinked star copolymer *via* redox reactions.

containing linear polymers above the CP *via* crosslinked disulfide bonds.

Inspired by our previous study[49] of the formation of microgels from thiol-containing linear P(NIPAM-*co*-MEA) chains by oxidative coupling using $K_3[Fe(CN)_6]$ in water at 45 °C, thiol-containing linear P(NIPAM-*co*-MEA)-*b*-PDMA obtained from the reductive cleavage of the disulfide-linked **HBP7-*star*-PDMA** polymer was further employed for the synthesis of core-crosslinked star polymer. Thiol-containing linear chains of P(NIPAM-*co*-MEA)-*b*-PDMA were self-assembled (Supporting Information, Fig. S11) above the CP of the PNIPAM-containg block, and star-shaped core-crosslinked star polymers were formed during subsequent oxidation with $K_3[Fe(CN)_6]$ (Scheme 4). The star formation process at 45 °C was monitored by SEC and DLS, as shown in Fig. 6(A) and 6(B). SEC indicated the formation of high molecular weight polymers (M_n = 2,270,000 g/mol), corresponding to core-crosslinked stars having a large number of arms, as compared to 49,300 g/mol for the linear P(NIPAM-*co*-MEA)-*b*-PDMA) starting materials obtained by formation of disulfide bonds in the self-assembled P(NIPAM-*co*-MEA)-*b*-PDMA polymers. Star formation was further confirmed by DLS (Fig. 6(B)), as the size of the polymers increased from 10 nm (linear segments) to 69 nm (star polymers) after oxidation. Fig. 6(C) shows that the hydrodynamic diameters of the star polymers at 25 and 45 °C are 69 and 58 nm, respectively, as a result of swelling and collapse of the PNIPAM chains in the crosslinked core. Fig. 6(D) shows the TEM images of core-crosslinked star polymers with average diameter of 49 nm. As expected, the size of the core-crosslinked star polymer by TEM measurement is smaller than that obtained by DLS results.[69] Oxidative coupling of thiol groups in linear P(NIPAM-*co*-MEA)-*b*-PDMA polymers was also studied in water at 25 °C for 24 h in the presence of $K_3[Fe(CN)_6]$. The SEC traces in Fig. 6(A) showed no significant shift to lower retention times, and no increase in size was observed by DLS (Fig. 6(B)), suggesting core crosslinking was inefficient under these conditions.

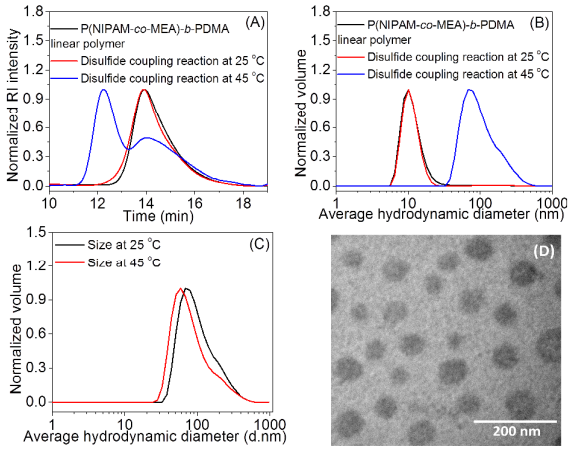

Fig. 6 (A) SEC-refractive index traces and (B) DLS solution size distribution showing formation of stars of linear P(NIPAM-*co*-MEA)-*b*-PDMA chain at 45 °C (blue line) and almost no star formation or coupling reactions between thiol groups between chains at 25 °C (red line). (C) Hydrodynamic radius of the star polymers in water below and above the CP. (D) TEM image of the disulfide core-crosslinked stars.

Conclusions

In summary, we successfully synthesized a series of thermo- and redox-responsive hyperbranched polymers with disulfide crosslinkers by RAFT. Polymerization kinetics indicated controlled synthesis of hyperbranched polymers was achieved by RAFT polymerization. The branch density in the resulting polymers was readily altered with variation of monomer and comonomer feed ratios. Branched P(NIPAM-*co*-BAC) was used as a macro-CTA for the synthesis of branched core-crosslinked star copolymers. The CP of P(NIPAM-*co*-BAC) was tuned by adjusting the feed ratio of NIPAM and BAC, and the CP was found to decrease with increasing number of hydrophobic branched units in the polymers. DLS results revealed that the aggregated size of branched polymer at the CP had a positive correlation with the average number of repeat units per branch. Reductive dissociation of disulfide-bonds in hyperbranched polymers yielded thiol-containing linear polymer chains, and oxidative reconstruction of the disulfide linkages produced the hyperbranched polymers reversibly. Re-formation of hyperbranched polymer by oxidation of thiol groups in P(NIPAM-*co*-MEA) was observed below the CP, but microgels formed above the CP. DLS and TEM results revealed that thiol-containing P(NIPAM-*co*-MEA)-*b*-PDMA formed core-

crosslinked star polymers by re-oxidation at 45 °C, whereas disulfide crosslinked polymers may have formed at 25 °C rather than branched or star polymers. Hyperbranched polymers are interesting architectures for a variety of applications, and the inclusion of two separate stimuli susceptibilities into a single branched polymer architecture may facilitate their utility in a number of emerging applications, including drug delivery, smart coatings, and self-healing materials.

Acknowledgements

This material is based upon work supported by the National Science Foundation [DMR-1410223 (B.S.S.) and DGE-1315138 (M.R.H.)].

Notes and references

1. A. Carlmark, C. Hawker, A. Hult and M. Malkoch, *Chem. Soc. Rev.*, 2009, 38, 352-362.
2. B. I. Voit and A. Lederer, *Chem. Rev.*, 2009, 109, 5924-5973.
3. R. M. England and S. Rimmer, *Polym. Chem.*, 2010, 1, 1533-1544.
4. S. Nayak and L. A. Lyon, *Angew. Chem. Int. Ed.*, 2004, 43, 6706-6709.
5. H.-s. Peng, J. A. Stolwijk, L.-N. Sun, J. Wegener and O. S. Wolfbeis, *Angew. Chem. Int. Ed.*, 2010, 49, 4246-4249.
6. T. C. Stover, Y. S. Kim, T. L. Lowe and M. Kester, *Biomaterials*, 2008, 29, 359-369.
7. R. B. Arote, E.-S. Lee, H.-L. Jiang, Y.-K. Kim, Y.-J. Choi, M.-H. Cho and C.-S. Cho, *Bioconjugate Chem.*, 2009, 20, 2231-2241.
8. J. Wang, K. P. Loh, Z. Wang, Y. Yan, Y. Zhong, Q.-H. Xu and P. C. Ho, *Angew. Chem. Int. Ed.*, 2009, 48, 6282-6285.
9. C. Gota, K. Okabe, T. Funatsu, Y. Harada and S. Uchiyama, *J. Am. Chem. Soc.*, 2009, 131, 2766-2767.
10. M. Bednarek, T. Biedron, J. Helinski, K. Kaluzynski, P. Kubisa and S. Penczek, *Macromol. Rapid Commun.*, 1999, 20, 369-372.
11. H. Magnusson, E. Malmström and A. Hult, *Macromol. Rapid Commun.*, 1999, 20, 453-457.
12. C. Gao and D. Yan, *Prog. Polym. Sci.*, 2004, 29, 183-275.
13. B. Liu, A. Kazlauciunas, J. T. Guthrie and S. Perrier, *Macromolecules*, 2005, 38, 2131-2136.
14. A. P. Vogt and B. S. Sumerlin, *Macromolecules*, 2008, 41, 7368-7373.
15. C. Walling, *J. Am. Chem. Soc.*, 1945, 67, 441-447.
16. R. H. Pelton and P. Chibante, *Colloids and Surf.*, 1986, 20, 247-256.
17. H. Gao and K. Matyjaszewski, *Prog. Polym. Sci.*, 2009, 34, 317-350.
18. J. M. J. Frechet, M. Henmi, I. Gitsov, S. Aoshima, M. R. Leduc and R. B. Grubbs, *Science (Washington, D. C.)*, 1995, 269, 1080-1083.
19. A. P. Vogt, S. R. Gondi and B. S. Sumerlin, *Aust. J. Chem.*, 2007, 60, 396-399.
20. S. Ghosh Roy and P. De, *Polym. Chem.*, 2014, 5, 6365-6378.
21. K. Matyjaszewski, S. G. Gaynor and A. H. E. Müller, *Macromolecules*, 1997, 30, 7034-7041.
22. K. Matyjaszewski, S. G. Gaynor, A. Kulfan and M. Podwika, *Macromolecules*, 1997, 30, 5192-5194.
23. H. Sun, C. P. Kabb and B. S. Sumerlin, *Chem.l Sci.*, 2014, 5, 4646-4655.
24. C. J. Hawker, J. M. J. Frechet, R. B. Grubbs and J. Dao, *J. Am. Chem. Soc.*, 1995, 117, 10763-10764.
25. Y. Tao, J. He, Z. Wang, J. Pan, H. Jiang, S. Chen and Y. Yang, *Macromolecules*, 2001, 34, 4742-4748.
26. D. Konkolewicz, A. Gray-Weale and S. Perrier, *Polym. Chem.*, 2010, 1, 1067-1077.
27. A. T. Slark, D. C. Sherrington, A. Titterton and I. K. Martin, *J. Mater. Chem.*, 2003, 13, 2711-2720.
28. F. Isaure, P. A. G. Cormack, S. Graham, D. C. Sherrington, S. P. Armes and V. Butun, *Chem. Commun.*, 2004, DOI: 10.1039/B401709A, 1138-1139.
29. F. Isaure, P. A. G. Cormack and D. C. Sherrington, *Macromolecules*, 2004, 37, 2096-2105.
30. N. O'Brien, A. McKee, D. C. Sherrington, A. T. Slark and A. Titterton, *Polymer*, 2000, 41, 6027-6031.
31. P. A. Costello, I. K. Martin, A. T. Slark, D. C. Sherrington and A. Titterton, *Polymer*, 2002, 43, 245-254.
32. S. R. Carter and S. Rimmer, *Polym. Prepr. (Am. Chem. Soc., Div. Polym. Chem.)*, 2002, 43, 1297-1298.
33. H. Wei, S.-X. Cheng, X.-Z. Zhang and R.-X. Zhuo, *Prog. Polym. Sci.*, 2009, 34, 893-910.
34. I. Dimitrov, B. Trzebicka, A. H. E. Müller, A. Dworak and C. B. Tsvetanov, *Prog. Polym. Sci.*, 2007, 32, 1275-1343.
35. M. Luzon, C. Boyer, C. Peinado, T. Corrales, M. Whittaker, L. Tao and T. P. Davis, *J. Polym. Sci. Part A: Polym. Chem.*, 2010, 48, 2783-2792.
36. S. J. Rowan, S. J. Cantrill, G. R. L. Cousins, J. K. M. Sanders and J. F. Stoddart, *Angew. Chem. Int. Ed.*, 2002, 41, 898-952.
37. P. T. Corbett, J. Leclaire, L. Vial, K. R. West, J.-L. Wietor, J. K. M. Sanders and S. Otto, *Chem. Rev.*, 2006, 106, 3652-3711.
38. A. Ciferri, *Supramolecular Polymers, Second Edition*, CRC Press, 2005.
39. J. Rosselgong and S. P. Armes, *Macromolecules*, 2012, 45, 2731-2737.
40. A. P. Bapat, D. Roy, J. G. Ray, D. A. Savin and B. S. Sumerlin, *J. Am. Chem.l Soc.*, 2011, 133, 19832-19838.
41. L. Li, X. Wang, J. Yang, X. Ye and C. Wu, *Macromolecules*, 2014, 47, 650-658.
42. M. L. Szalai, D. V. McGrath, D. R. Wheeler, T. Zifer and J. R. McElhanon, *Macromolecules*, 2007, 40, 818-823.
43. K. Wang, H. Peng, K. J. Thurecht, S. Puttick and A. K. Whittaker, *Polym. Chem.*, 2014, 5, 1760-1771.
44. R. Deng, Y. Yue, F. Jin, Y. Chen, H.-F. Kung, M. C. M. Lin and C. Wu, *J. Controlled Release*, 2009, 140, 40-46.
45. W. Wang, H. Sun, F. Meng, S. Ma, H. Liu and Z. Zhong, *Soft Matter*, 2012, 8, 3949-3956.
46. J.-H. Ryu, R. T. Chacko, S. Jiwpanich, S. Bickerton, R. P. Babu and S. Thayumanavan, *J. Am. Chem. Soc.*, 2010, 132, 17227-17235.
47. G. Deng, F. Li, H. Yu, F. Liu, C. Liu, W. Sun, H. Jiang and Y. Chen, *ACS Macro Lett.*, 2012, 1, 275-279.
48. Y. Chu, H. Yu, Y. Ma, Y. Zhang, W. Chen, G. Zhang, H. Wei, X. Zhang, R. Zhuo and X. Jiang, *J. Polym. Sci. Part A: Polym. Chemi.*, 2014, 52, 1771-1780.

49. A. P. Bapat, J. G. Ray, D. A. Savin and B. S. Sumerlin, *Macromolecules*, 2013, 46, 2188-2198.
50. L. E. Overman, J. Smoot and J. D. Overman, *Synthesis*, 1974, DOI: 10.1055/s-1974-23245, 59-60.
51. S. Singh, F. Topuz, K. Hahn, K. Albrecht and J. Groll, *Angew. Chem. Int. Ed.*, 2013, 52, 3000-3003.
52. A. P. Vogt and B. S. Sumerlin, *Soft Matter*, 2009, 5, 2347-2351.
53. M. R. Whittaker, Y.-K. Goh, H. Gemici, T. M. Legge, S. Perrier and M. J. Monteiro, *Macromolecules*, 2006, 39, 9028-9034.
54. B. T. Michal, C. A. Jaye, E. J. Spencer and S. J. Rowan, *ACS Macro Lett.*, 2013, 2, 694-699.
55. J. Zhang, F. Yang, H. Shen and D. Wu, *ACS Macro Lett.*, 2012, 1, 1295-1299.
56. N. Morimoto, X.-P. Qiu, F. M. Winnik and K. Akiyoshi, *Macromolecules*, 2008, 41, 5985-5987.
57. H. Kang, A. C. Trondoli, G. Zhu, Y. Chen, Y.-J. Chang, H. Liu, Y.-F. Huang, X. Zhang and W. Tan, *ACS Nano*, 2011, 5, 5094-5099.
58. T. Xing, C. Mao, B. Lai and L. Yan, *ACS Appl. Mater. & Interfaces*, 2012, 4, 5662-5672.
59. Y. Zhuang, Y. Su, Y. Peng, D. Wang, H. Deng, X. Xi, X. Zhu and Y. Lu, *Biomacromolecules*, 2014, 15, 1408-1418.
60. S. Kumar, S. G. Roy and P. De, *Polym. Chem.*, 2012, 3, 1239-1248.
61. Y.-M. Bao, X.-H. Liu, X.-L. Tang and Y.-S. Li, *Journal of Polymer Science Part A: Polym. Chem.*, 2010, 48, 5364-5374.
62. Y. Segawa, T. Higashihara and M. Ueda, *J. Am. Chem. Soc.*, 2010, 132, 11000-11001.
63. Z. Wei, X. Hao, P. A. Kambouris, Z. Gan and T. C. Hughes, *Polymer*, 2012, 53, 1429-1436.
64. D. Yan, A. H. E. Müller and K. Matyjaszewski, *Macromolecules*, 1997, 30, 7024-7033.
65. C. J. Hawker, R. Lee and J. M. J. Frechet, *J. Am. Chem. Soc.*, 1991, 113, 4583-4588.
66. Y. Chen, K. Fuchise, A. Narumi, S. Kawaguchi, T. Satoh and T. Kakuchi, *Macromolecules*, 2011, 44, 9091-9098.
67. X. Xia, Z. Ye, S. Morgan and J. Lu, *Macromolecules*, 2010, 43, 4889-4901.
68. W. Zhang, X. Zhou, H. Li, Y. Fang and G. Zhang, *Macromolecules*, 2005, 38, 909-914.
69. H. Huang, E. E. Remsen, T. Kowalewski and K. L. Wooley, *J. Am. Chem. Soc.*, 1999, 121, 3805-3806.